



Received on 22 May, 2016; received in revised form, 02 September, 2016; accepted, 23 September, 2016; published 01 October, 2016

## SELF-ASSEMBLED BIODEGRADABLE POLYMERIC NANOPARTICLES WITH IMPROVED SOLUBILITY OF CARVEDILOL: PREPARATION, CHARACTERISATION AND *IN VITRO* RELEASE KINETICS

Shahzeb Khan<sup>1</sup>, Waqar Ali<sup>2</sup>, Nisar Ur Rahman<sup>2</sup>, Syed Muhammad Mukarram Shah<sup>1</sup>, Jahangir Khan<sup>1</sup>, Syed Muhammad Hassan Shah<sup>3</sup>, Zahid Hussain<sup>\*4</sup>

Department of Pharmacy<sup>1</sup>, University of Malakand Dir Lower, Khyber Pakhtunkhwa, Pakistan.

Faculty of Pharmacy<sup>2</sup>, COMSATS Institute of Information Technology (CIIT), Abbottabad Campus, Khyber Pakhtunkhwa, Pakistan.

Department of Pharmacy<sup>3</sup>, Sarhad University, Khyber Pakhtunkhwa, Peshawar, Pakistan.

Department of Pharmaceutics<sup>4</sup>, Faculty of Pharmacy, Universiti Teknologi MARA, Puncak Alam Campus, Bandar Puncak Alam, 42300, Selangor, Malaysia.

### Keywords:

Poly(lactide-co-glycolide)/poly (lactide-co-glycolide)-poly (ethylene glycol) nanoparticles; Particle size and zeta potential; Surface morphology; Improved solubility; *In vitro* release kinetics

### Correspondence to Author:

**Dr. Zahid Hussain**


Department of Pharmaceutics,  
Faculty of Pharmacy, Universiti  
Teknologi MARA, Puncak Alam  
Campus, Bandar Puncak Alam,  
42300, Selangor, Malaysia.

**Email:** zahidh85@yahoo.com

**ABSTRACT:** Nanoparticles (NPs) have been extensively studied during the past few decades due to their well-recognised applicability. Thus, the present study was aimed to fabricate Carvedilol (CVD) a  $\beta$ -adrenoceptor antagonist, as NPs aiming towards the optimal physicochemical characteristics and improved solubility. The prepared NPs demonstrated a linear increase in the mean particle size from  $253 \pm 19$  to  $598 \pm 21$  nm and entrapment efficiency (%EE) from 58.6% to 91.1%, when drug-to-polymer mass ratio was increased from 1:1 to 1:5. *In vitro* release studies showed significant variation in the rate and extent of CVD release from polymeric matrix at various pHs of release media (pH 1.2, pH 6.8 and distilled water) and drug-to-polymer mass ratios. The present study highlighted the optimal formulation conditions to fabricate CVD-loaded NPs with best physicochemical characteristics, improved solubility of incorporated drug and explored the prospects of manipulation and optimisation of the NPs for intended applications.

**INTRODUCTION:** It has been reported that approximately 40% and even greater number of active pharmaceutical ingredients (APIs) being recognized *via* combinatory screening programmed are poor water soluble.

Solubility, dissolution and eventually gastrointestinal permeability are the major factors which determine the bioavailability and absorption of a drug. However, a number of drugs under investigation have poor aqueous solubility and potentially this can lead to a more striking situation in the future. Over the past few decades, nanoparticles (NPs) have been gaining momentum to tackle problems associated with poor solubility and low bioavailability and significantly improved therapeutic potential of pharmacological moieties. An optimum reduction in the particle size of NPs could lead to a substantial increase in the

<b>QUICK RESPONSE CODE</b> 	<b>DOI:</b> 10.13040/IJPSR.0975-8232.7(10).3971-85
	<b>Article can be accessed online on:</b> <a href="http://www.ijpsr.com">www.ijpsr.com</a>
<b>DOI link:</b> <a href="http://dx.doi.org/10.13040/IJPSR.0975-8232.7(10).3971-85">http://dx.doi.org/10.13040/IJPSR.0975-8232.7(10).3971-85</a>	

dissolution rate of a drug which in turn could result in marked increases in oral bioavailability<sup>1</sup>. The recent approaches used to prepare drug-loaded NPs can be classified into two main categories: top down and bottom up approaches<sup>2</sup>. The top down method refers a technique of producing NPs from the larger micro particles *via* disintegration or breaking agglomeration. This technique includes high pressure homogenization and media milling method<sup>3</sup>. In contrast the bottom up approach involves the aggregation of molecules to nano-range sized particles such as micro-emulsion, micro-precipitation and melt-emulsification methods<sup>3</sup>.

Among several biodegradable polymers, poly (D,L-lactic acid) (PLA), poly(D,L-lactic-co-glycolic acid) (PLGA) and poly(3-caprolactone) have received a noticeable attraction in drug delivery<sup>4-6</sup>. These biodegradable polymers and their co-polymers diblocked or multiblocked with PEG have been commonly used to form core-shell structured NPs to encapsulate a variety of therapeutic compounds<sup>7-10</sup>. These NPs have a number of appealing features: their hydrophobic core is capable of carrying highly insoluble drugs with high loading capacity, while their hydrophilic shell provides steric protection and functional groups for surface modification. Drug release can be manipulated by choosing biodegradable polymers with different surface or bulk erosion rates, and external conditions such as pH and temperature changes may function as a switch to trigger drug release<sup>11, 12</sup>. However to date polymeric NPs have shown moderate circulation half-lives compared to their liposomal counterparts, which could be modified *via* coating with inert and biocompatible polymers such as polyethylene glycol (PEG)<sup>13</sup>.

Ethyl cellulose (EC), being semi synthetic material and exhibiting promising features of biocompatibility and biodegradability, has been studied extensively in the preparation of drug carrying nano-carriers. Owing to poor water solubility its use in various fields has however been declined. PEG which is an inert, biodegradable and biocompatible polymer has some other paramount pharmaceutical attributes which include hydrophilic nature and low intrinsic toxicity and has gained remarkable attention in recent few decades to shield encapsulated drugs and to coat

less water soluble polymer to reduce systemic clearance rate and prolong circulation half-life *in vivo*<sup>14, 15</sup>. The high hydrophilic nature of PEG enhances the solubility of hydrophobic drugs or carriers when conjugated with them. One of the useful strategies for modifying the physicochemical and biological properties of hydrophobic and biodegradable PLGA has been to incorporate hydrophilic PEG segments. PLGA-PEG block copolymers became a new family of biomaterials with their own unique properties including microphase separation, crystallinity, water-solubility, and biodegradability.

Carvedilol (CVD) is a nonselective  $\beta$ -adrenoceptors and  $\alpha$ -adrenoceptors blocker and exhibits strong blood pressure lowering effects *via* vasodilatation and reduction in heart contractility. The chemical structure of CVD is shown in **Fig. 1**. CVD belongs to BCS II class of drug compounds which have high permeability but poor water solubility. Therefore the oral bioavailability of CVD accounts only 25 to 35% because of slow rate of dissolution and a high grade of first pass metabolism<sup>2</sup>. Lower dissolution and poor solubility eventually would result in variable and erratic absorption in gastrointestinal tract following oral administration<sup>16</sup>.

This critical issue has been a major hindrance in drug development. The poor water solubility issue followed by a low bioavailability has been frequently reported for the drugs which are being administered *via* oral route<sup>17, 18</sup>. Formulation strategies for overcoming dissolution-related problems of CVD include: use of lipophilic solutions, salt form of drug, formation of inclusion complex with cyclodextrin, use of self-emulsifying system, and preparation of CVD-loaded polymeric NPs using anti-solvent precipitation-ultrasonication method.

Herein we report the systematic preparation and characterization of CVD-loaded EC-, PEG- and PLGA-PEG diblock copolymer based NPs. We evaluated parameters that could influence core-shell nanostructure to find an optimal formulation, physicochemical characteristics, morphological attributes, and *in vitro* release profile. The major focus of the present study was the optimization of solubility and dissolution of CVD by fabricating in

various biocompatible and biodegradable polymers and to evaluate their potentials to enhance the rate and extent drug absorption through the oral route.

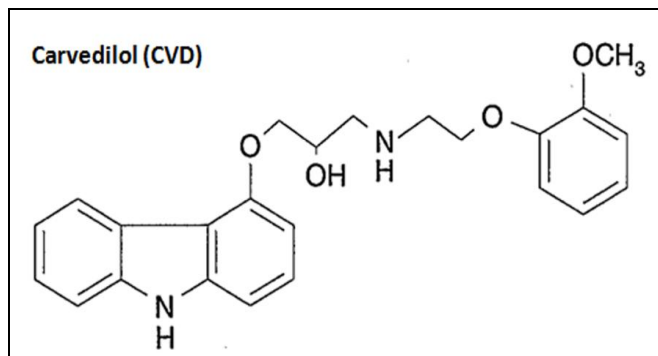


FIG. 1: CHEMICAL STRUCTURE OF CARVEDILOL (CVD).

## 2. MATERIALS AND METHODS:

**2.1. Materials:** Polylactic acid co-glycolic acid (PLGA 75:25) was purchased from Ivomec USA. Polyethylene glycol (PEG 8000), Ethyl cellulose (EC), Polyvinyl alcohol (MW 30-70 kDa), dichloromethane was purchased from Sigma Aldrich, Malaysia. Carvedilol (CVD) was sourced as a sample from Feroz Sons laboratory Nowshera, Pakistan. All other chemicals used were of analytical grade and were sourced from laboratories of Universiti Teknologi MARA, Malaysia.

**2.2. Preparation of CVD-loaded EC-NPs, -PEG-NPs and -PLGA-PEG-NPs:** To prepare CVD-loaded-EC-NPs, -PEG-NPs, -PLGA-PEG-NPs, CVD and polymer (EC, PEG, PLGA-PEG-diblock copolymers) were dissolved in dichloromethane with various drug-to-polymer mass ratios (1:1, 1:2.5, and 1:5). The individual drug-polymer solution was then introduced into the aqueous solution of PVA dropwise under constant magnetic stirring to form emulsion (o/w). The resulting emulsion was stirred at 1000 rpm for 20 min and was subsequently homogenised at 25000 rpm for 5 min using a high speed homogenizer. Afterward, the homogenized emulsion was diluted with equivalent volume of aqueous solution of PVA and was stirred for 24 h under fume hood to allow diffusion of dichloromethane to aqueous phase. After an efficient removal of residual organic solvent under fume hood, unwanted small particles were removed by centrifugation at 10,000 rpm for 10 min. The resulted EC-NPs, PEG-NPs or PLGA-PEG-NPs were harvested by ultra-centrifugation at 28000 rpm using an Optima L-100 XP Ultracentrifuge (Beckman-Coulter, USA) with a

NV 70.1 Ti rotor (Beckman-Coulter, USA) for 30 min. Afterward, the NPs sediment and supernatant were separated carefully by removing supernatant layer and the NPs were washed thrice to remove any traces of PVA prior to lyophilisation (Scanvac Cool Safe™, Chemoscience, Thailand) at -40 °C for 24 h for further evaluation.

We investigated the effect of several parameters on the physico-chemical characteristics of prepared polymeric NPs. In the first set of experiments, we used different mass ratios of three polymers (EC, PEG, PLGA-PEG diblock copolymers) with CVD as: 1:1 (CVD: EC/PEG/PLGA-PEG), 1:2.5 (CVD: EC/PEG/PLGA-PEG) and 1:5 (CVD: EC/PEG/PLGA-PEG) and characterized them for mean particle size, zeta potential, polydispersity index (PDI), entrapment efficiency (%EE) and loading contents (%LC). In the second set of experiments we evaluated the effect of various types of polymer on the characteristics FT-IR spectra, morphology, and *in vitro* release kinetics.

**2.2. Characterization of CVD-loaded EC-NPs, -PEG-NPs and -PLGA-PEG-NPs:** The sediment pellets of loaded NPs (CVD-loaded-EC-NPs, -PEG-NPs and -PLGA-PEG-NPs) obtained after ultra-centrifugation were resuspended and dispersed in distilled water. To further improve the dispersion and segregation of particulate aggregates, the Nano-suspension was stirred at 2000 rpm using magnetic stirrer for 10 min. The resulting Nano-suspensions were then subjected to ZS-90 Zetasizer® (Malvern Instruments Ltd., UK) to measure the mean particle size, zeta potential and PDI using the dynamic light scattering technique. All measurements were performed in triplicates at 25°C with a detection angle of 90°. Results were reported as mean ± standard deviation (S.D.) (n=3).

**2.3. Measurement of %EE and %LC:** To measure the %EE and %LC of CVD in CVD-loaded-EC-NPs, -PEG-NPs and -PLGA-PEG-NPs, the corresponding standard calibration curve was made by subjecting various standard solutions CVD (1 to 1000µg/mL) to UV-visible spectrophotometer. The characteristic peak of CVD was measured at 286 nm. The %EE and %LC of CVD were calculated using equation 1 and 2 respectively,<sup>19</sup>.



$$EE (\%) = W_t - W_f / W_t \times 100 \quad (\text{Equation 1})$$

$$LC (\%) = W_t - W_f / W_n \times 100 \quad (\text{Equation 2})$$

Where,  $W_t$  is the total initial amount of CVD and  $W_f$  is the amount of free drug in the supernatant after ultracentrifugation.  $W_n$  is the average weight of lyophilized CVD-loaded NPs obtained from all polymers. All measurements were performed in triplicate and were reported as mean  $\pm$  S.D (n = 3).

**2.4. Morphological examination using Scanning Electron Microscopy (SEM):** To evaluate the effect of using various polymers (EC, PEG, and PLGA-PEG) on the morphological characteristics, the prepared CVD-loaded NPs (-EC-NPs, -PEG-NPs and -PLGA-PEG-NPs) were visualized under Scanning Electron Microscope (SEM) (Nova Nano SEM, USA). The experiment was performed at an accelerating voltage of 10-15 kV and a secondary detector. The fresh sample of each Nano-suspension aliquot was placed on a glass slide which was coated with gold and dried in desiccators before microscopic analyses. Subsequently the dried gold-plated micro grids were viewed under different resolutions of SEM.

**2.6. Fourier Transform Infrared Spectrophotometric (FT-IR) Analysis:** The Fourier transform infrared (FT-IR) spectra were scanned using IR Affinity-1S FT-IR spectrophotometer (SHIMADZU, Japan). Briefly, a small quantity (2–3 mg) of CVD, EC and CVD-loaded EC-NPs were mixed with 200–300 mg potassium bromide (KBr) separately and were compressed to form transparent pellets using a hydraulic press. Notably prior to form transparent pellets, the materials were dried in oven overnight. Similar procedures were used to prepare transparent pellets of PEG, CVD-loaded PEG-NPs, PLGA-PEG diblock copolymer and CVD-loaded PLGA-PEG-NPs. Finally, the resulting pellets were scanned in transmission mode in a spectral region of 4000–500  $\text{cm}^{-1}$  using a resolution of 1  $\text{cm}^{-1}$  and 32 co-added scans. The FT-IR data were analyzed by using Origin 6.1 software to find characteristic peaks.

**2.7. *In vitro* release kinetic studies:** In this set of experiments, *in vitro* dissolution studies were carried out by using USP dissolution apparatus II maintained at  $37 \pm 0.5^\circ\text{C}$  with stirring rate of 50

rpm. In doing so, accurately weighed bulk CVD and CVD-loaded EC-NPs, -PEG-NPs and -PLGA-PEG-NPs (amount equivalent to 12 mg of CVD) were dispersed in 500 mL of buffer dissolution media at pH 1.2, 6.8 and water. At predetermined time points (5, 10, 15, 30, 45 and 60 min), 5 mL of dissolution media was drawn and supplemented with equivalent volume of fresh dissolution media. Afterward, the samples were filtered using filter paper and the drug contents were measured by using UV-visible spectrophotometer at 286 nm. All measurements were performed in triplicate and data was reported as mean  $\pm$  S.D (n = 3).

**2.8. Statistical data analysis:** All the data is presented as mean  $\pm$  S.D (n=3). Data were analyzed using either paired t-tests or independent t-test and analysis of variance (ANOVA). For the data obtained from the mean particle size, zeta potential, PDI, %EE, %LC and *in vitro* release studies, a *p* value  $< 0.05$  was considered to indicate a significant difference between the samples tested.

### 3. RESULTS AND DISCUSSION:

**3.1. Determination of mean particle size (nm):** The mean particle sizes of CVD-loaded EC-NPs, -PEG-NPs, and -PLGA-PEG-NPs with varying drug-to-polymer mass ratios (1:1, 1:2.5 and 1:5) are shown in **Table 1**. The data obtained highlighted that the mean particle size of CVD-loaded EC-NPs was significantly ( $p < 0.05$ , paired t-test) increased from  $209 \pm 16$  nm to  $412 \pm 26$  nm by varying drug-to-polymer mass ratio from 1:1 (CVD: EC) to 1: 5. The CVD-loaded EC-NPs showed relatively narrow size distribution index (PDI) of  $0.23 \pm 0.04$  to  $0.41 \pm 0.09$  at various drug-to-polymer mass ratios. The authors of the present study also noticed similar increasing trends in the mean particle sizes of CVD-loaded-PEG- and CVD-loaded-PLGA-PEG-NPs, when the drug-to-polymer mass ratio was increased from 1:1 to 1:5 as shown in **Fig. 2**.

The mean particle sizes of CVD-loaded PEG-NPs and -PLGA-PEG-NPs were significantly ( $p < 0.05$ , paired t-test) increased from  $229 \pm 26$  nm and  $253 \pm 19$  nm to  $488 \pm 19$  nm and  $598 \pm 21$  nm when increasing the drug-to-polymer mass ratio from 1:1 to 1:5, respectively. On the other hand, the resulting data also revealed a considerable increase in the mean particle size of CVD-loaded NPs when prepared with different types of polymers. The

smallest mean particle size of  $209 \pm 16$  nm was produced by using EC and highest particle size of  $253 \pm 19$  nm was obtained when diblock copolymer (PLGA-PEG) was used to produce NPs at 1:1 drug-to-polymer mass ratios. Similar diversity in mean particle size was also observed when the CVD-loaded NPs were prepared on drug-to-polymer

mass ratios of 1:2.5 and 1:5 with all types of polymer as drug delivery systems. These results were also in agreement with previously published studies<sup>20, 21</sup>. The size distribution index of CVD-loaded NPs prepared from various polymers and on various drug-to-polymers mass ratios have been shown in **Fig.2**.

**TABLE 1: EFFECT OF DRUG-TO-POLYMER MASS RATIOS AND TYPES OF POLYMERS ON THE MEAN PARTICLE SIZE AND POLYDISPERSITY INDEX OF CVD-LOADED EC-NPs, -PEG-NPs, -PLGA-PEG-NPs.**

Formulation code	Drug-loaded Nanoparticles	Type of polymer	Drug-to-polymer mass ratio	Mean particle size (nm) $\pm$ SD	Polydispersity Index (PDI)
F1	CVD-EC-NPs	EC	1:1	$209 \pm 16$	$0.23 \pm 0.04$
	CVD-PEG-NPs	PEG	1:1	$229 \pm 26$	$0.31 \pm 0.06$
	CVD-PLGA-PEG-NPs	PLGA-PEG-diblock copolymer	1:1	$253 \pm 19$	$0.41 \pm 0.09$
F2	CVD-EC-NPs	EC	1:2.5	$254 \pm 18$	$0.34 \pm 0.1$
	CVD-PEG-NPs	PEG	1:2.5	$325 \pm 32$	$0.26 \pm 0.09$
	CVD-PLGA-PEG-NPs	PLGA-PEG-diblock copolymer	1:2.5	$387 \pm 27$	$0.42 \pm 0.03$
F3	CVD-EC-NPs	EC	1:5	$412 \pm 26$	$0.46 \pm 0.06$
	CVD-PEG-NPs	PEG	1:5	$488 \pm 19$	$0.53 \pm 0.09$
	CVD-PLGA-PEG-NPs	PLGA-PEG-diblock copolymer	1:5	$598 \pm 21$	$0.61 \pm 0.15$

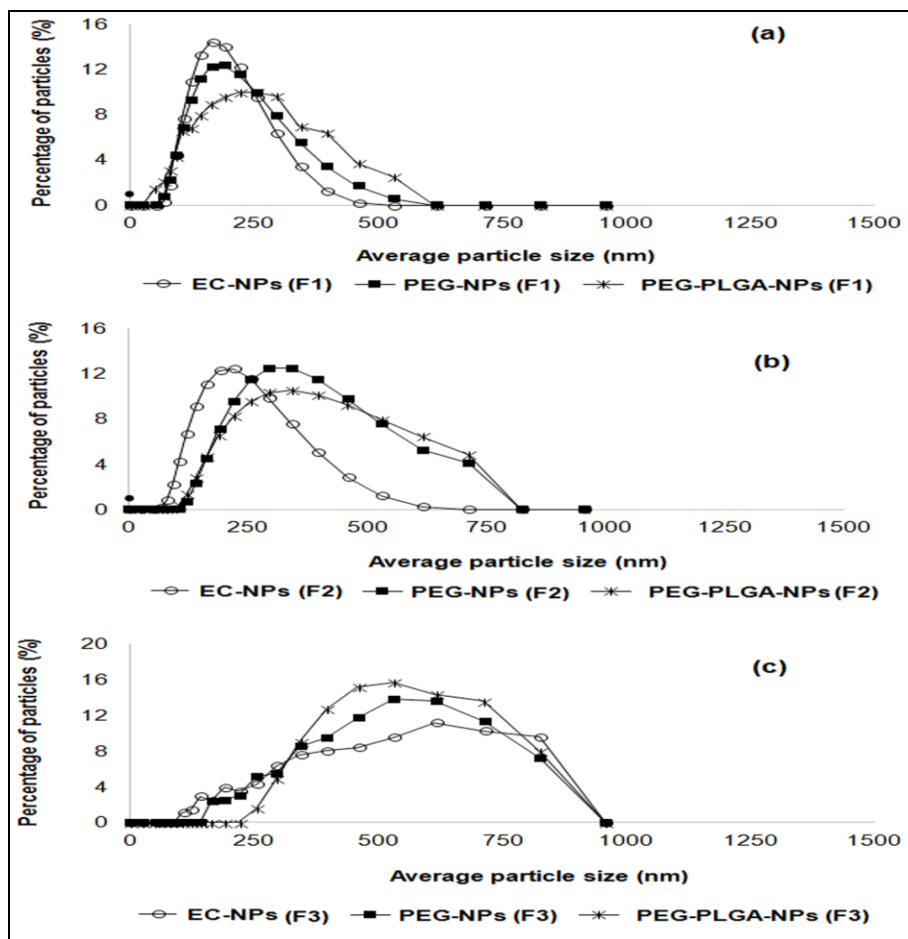


**FIG.2: EFFECT OF DRUG-TO-POLYMER MASS RATIO AND TYPE OF POLYMER ON (A) PARTICLE SIZE DISTRIBUTION OF EC-NPs, PEG-NPs AND PLGA-PEG-NPs AT 1:1 (F1), (B) PARTICLE SIZE DISTRIBUTION OF EC-NPs, PEG-NPs AND PLGA-PEG-NPs AT 1:2.5 (F2), AND (C) PARTICLE SIZE DISTRIBUTION OF EC-NPs, PEG-NPs AND PLGA-PEG-NPs AT 1:5 (F3).**

**3.2. Determination of average zeta potential (mV) of CVD-loaded NPs:** In the current experiment, the analysis of zeta potential was executed to evaluate the colloidal stability of the CVD-loaded EC-NPs, -PEG-NPs, and -PLGA-PEG-NPs. Many researchers investigated that the NPs with zeta potential values greater than +25 mV or less than -25 mV typically have higher degrees of colloidal stability in liquid formulations. The resulting data for the zeta potential of CVD-loaded EC-NPs, -PEG-NPs, and -PLGA-PEG-NPs with varying drug-to-polymer mass ratios has been shown in **Table 2**. Moreover **Fig.3** shows zeta potential values of the produced NPs.

Data obtained clearly highlighted that no significant ( $p>0.05$ , paired t-test) difference was observed in the zeta potential of CVD-loaded EC-NPs produced at various drug-to-polymer mass ratios. The zeta potential of EC-NPs was varied from  $-26.30 \pm -4.2$  mV to  $-27.93 \pm -4.2$  mV when the drug-to-polymer mass ratio was increased from 1:1 to 1:5 as shown in **Table 2**.

However there was observed a linear decrease in the zeta potential of CVD-loaded PEG-NPs from  $-11.08 \pm -1.8$  mV to  $-4.56 \pm -0.8$  mV when the drug-to-polymer mass ratio was increased from 1:1 to 1:5 respectively. Similarly a decreasing trend in the zeta potential of CVD-loaded PLGA-PEG-NPs was also observed when the drug-to-polymer mass ratio

was increased as shown in **Table 2**. Further screening of the obtained data explored a significant difference in the zeta potential of CVD-loaded NPs prepared using different polymers. The lowest zeta potential of  $-11.08 \pm -1.8$  mV was observed in case of CVD-loaded PEG-NPs compared to highest value of zeta potential ( $-54.26 \pm -7.2$  mV) observed in CVD-loaded PLGA-PEG-NPs. The higher value of zeta potential could impart greater colloidal stability to CVD-loaded PLGA-PEG-NPs in liquid formulation on storage. The greatly high zeta potential of CVD-loaded PLGA-PEG-NPs was expected to be caused by a balance between hydrophilic and hydrophobic component of a diblock copolymer (PLGA-PEG). PEG is hydrophilic, while PLGA is hydrophobic, combination of which tend to give stable nanoparticle.

In PEG-NPs zeta potential was observed to be less which might cause higher rate of aggregation. However NPs produced by copolymerization of PEG and PLGA showed higher zeta potential which can potentially exhibit greater colloidal stability. The high zeta potential of CVD-loaded PLGA-PEG-NPs could be attributed mainly to the adsorption of polyvinyl alcohol (PVA) onto the surface of particles which would promisingly improve stability of the CVD-loaded PLGA-PEG-NPs<sup>1</sup>.

**TABLE 2: EFFECT OF DRUG-TO-POLYMER MASS RATIOS AND TYPES OF POLYMERS ON THE AVERAGE ZETA POTENTIAL OF CVD-LOADED EC-NPs, -PEG-NPs, -PLGA-PEG-NPs.**

Formulation code	Drug-loaded Nanoparticles	Type of polymer	Drug-to-polymer mass ratio	Average zeta potential (mV) $\pm$ SD
<b>F1</b>	CVD-EC-NPs	EC	1:1	$-26.30 \pm -4.2$
	CVD-PEG-NPs	PEG	1:1	$-11.08 \pm -1.8$
	CVD-PLGA-PEG-NPs	PLGA-PEG-diblock copolymer	1:1	$-54.26 \pm -7.2$
<b>F2</b>	CVD-EC-NPs	EC	1:2.5	$-23.53 \pm -6.2$
	CVD-PEG-NPs	PEG	1:2.5	$-8.74 \pm -2.3$
	CVD-PLGA-PEG-NPs	PLGA-PEG-diblock copolymer	1:2.5	$-54.01 \pm -7.4$
<b>F3</b>	CVD-EC-NPs	EC	1:5	$-27.93 \pm -4.2$
	CVD-PEG-NPs	PEG	1:5	$-4.56 \pm -0.8$
	CVD-PLGA-PEG-NPs	PLGA-PEG-diblock copolymer	1:5	$-38.26 \pm -4.7$

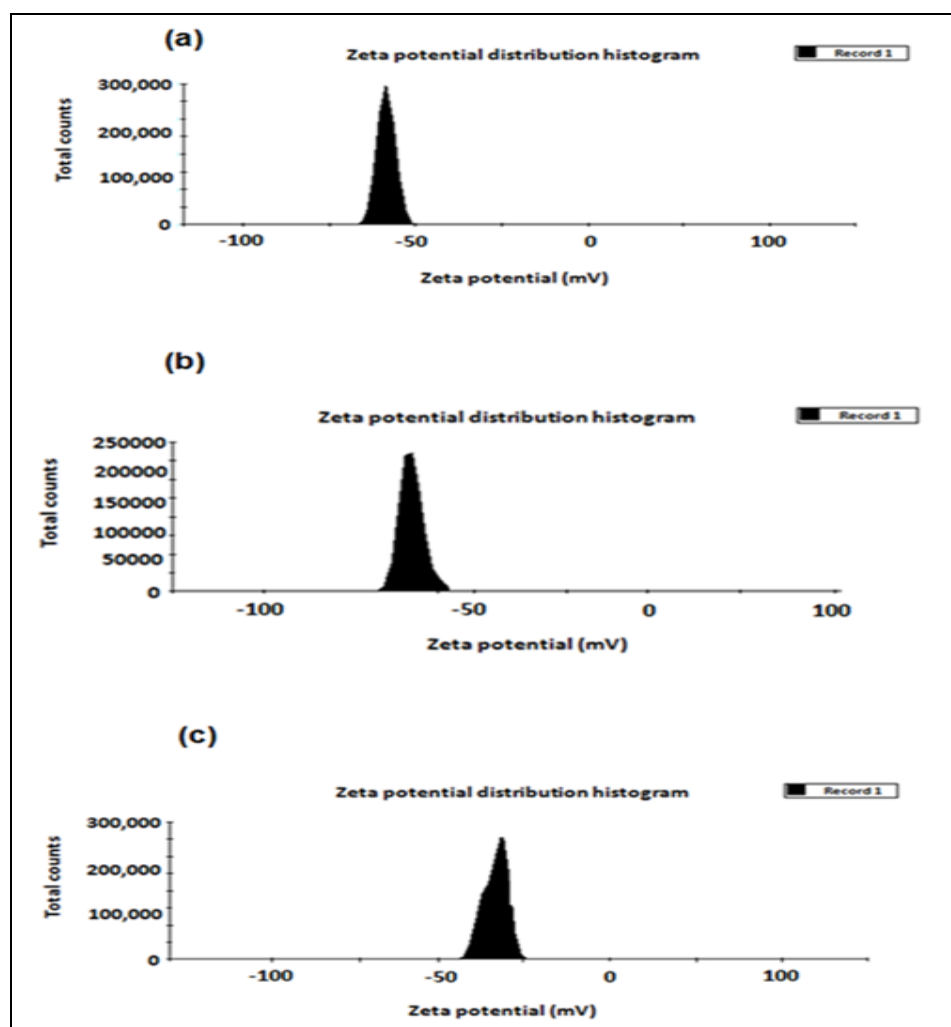


FIG. 3: EFFECT OF DRUG-TO-POLYMER MASS RATIOS ON THE ZETA POTENTIAL OF CVD-LOADED PLGA-PEG-NPs (A) ZETA POTENTIAL DISTRIBUTION HISTOGRAM OF PLGA-PEG-NPs AT 1:1 (SHOWING APPROX. -54.2 mV), (b) ZETA POTENTIAL DISTRIBUTION HISTOGRAM OF PLGA-PEG-NPs AT 1:2.5 (SHOWING APPROX. -54.4 mV), (c) ZETA POTENTIAL DISTRIBUTION HISTOGRAM OF PLGA-PEG-NPs AT 1:5 (SHOWING APPROX. -38 mV).

**3.3. Measurement of % EE and % LC:** The % EE and % LC of the CVD-loaded EC-NPs, -PEG-NPs, and -PLGA-PEG-NPs with varying drug-to-polymer mass ratios (1:1, 1:2.5 and 1:5) are presented in **Table 3**. It became evident from the obtained data that the % EE of CVD-loaded EC-NPs was significantly ( $p < 0.05$ , paired t-test) increased from  $28.56 \pm 4.2\%$  to  $66.57 \pm 9.4\%$  by increasing drug-to-polymer ratio from 1:1 to 1: 5 (**Table 3**). Similarly by increasing the drug-to-polymer mass ratios from 1:1 to 1:5, the % EE of CVD-loaded PEG-NPs and PLGA-PEG-NPs was increased from  $40.10 \pm 5.6\%$  to  $60.21 \pm 8.5\%$  and  $58.6 \pm 9.1\%$  to  $91.10 \pm 7.4\%$  respectively. These results were also in accordance with previously published studies<sup>22, 23</sup>. Despite that a significant ( $p < 0.05$ , paired t-test) variation in % EE was also observed by using different polymer types in producing CVD-loaded NPs at the same drug-to-

polymer mass ratios as shown in **Table 3**. The % EE of CVD was however found to be significantly improved from  $28.56 \pm 4.2\%$  to  $58.6 \pm 9.1\%$  when the drug was loaded onto EC-NPs, PEG-NPs and PLGA-PEG-NPs respectively at 1:1 drug-to-polymer mass ratio. Similar increasing trend in % EE of CVD was also observed on other drug-to-polymer mass ratios as shown in **Table 3**.

Moreover the data also demonstrated that % LC of CVD-loaded EC-NPs was significantly ( $p < 0.05$ , paired t-test) increased from  $19.14 \pm 3.2\%$  to  $35.69 \pm 4.2\%$  when the drug-to-polymer mass ratio was increased from 1:1 to 1: 5(**Table 3**). Similarly % LC of CVD-loaded PEG-NPs was also observed to be increased from  $31.45 \pm 2.4\%$  to  $56.89 \pm 8.4\%$  and for CVD-loaded PLGA-PEG-NPs was increased from  $28.41 \pm 5.2\%$  to  $57.65 \pm 6.3\%$ , when the drug-to-polymer mass ratios were



increased from 1:1 to 1:5, respectively. The data shown in **Table 3** demonstrates that there was observed a significant ( $p < 0.05$ , paired t-test) variation in % LC while using the same drug to polymer mass ratio of different polymers to produce CVD-loaded NPs. The % LC of CVD was found to be significantly improved from  $19.14 \pm$

$3.2\%$  to  $28.41 \pm 5.2\%$  when was loaded onto EC-NPs, PEG-NPs and PLGA-PEG-NPs respectively at 1:1 drug-to-polymer mass ratio. Similar increasing trend in % LC of CVD was also observed when other drug-to-polymer mass ratios were used to produce CVD-loaded NPs as shown in **Table 3**.

**TABLE 3: EFFECT OF DRUG-TO-POLYMER MASS RATIOS AND TYPES OF POLYMERS ON THE % EE AND % LC OF CVD IN CVD-LOADED EC-NPs, -PEG-NPs, -PLGA-PEG-NPs.**

Formulation code	Drug-loaded Nanoparticles	Type of polymer	Drug-to-polymer mass ratio	EE (%) $\pm$ SD	LC (%) $\pm$ SD
<b>F1</b>	CVD-EC-NPs	EC	1:1	$28.56 \pm 4.2$	$19.14 \pm 3.2$
	CVD-PEG-NPs	PEG	1:1	$40.10 \pm 5.6$	$31.45 \pm 2.4$
	CVD-PLGA-PEG-NPs	PLGA-PEG-diblock copolymer	1:1	$58.6 \pm 9.1$	$28.41 \pm 5.2$
<b>F2</b>	CVD-EC-NPs	EC	1:2.5	$45.61 \pm 5.5$	$27.33 \pm 2.5$
	CVD-PEG-NPs	PEG	1:2.5	$56.66 \pm 6.1$	$47.22 \pm 7.2$
	CVD-PLGA-PEG-NPs	PLGA-PEG-diblock copolymer	1:2.5	$76.32 \pm 8.7$	$50.56 \pm 5.3$
<b>F3</b>	CVD-EC-NPs	EC	1:5	$66.57 \pm 9.4$	$35.69 \pm 4.2$
	CVD-PEG-NPs	PEG	1:5	$60.21 \pm 8.5$	$56.89 \pm 8.4$
	CVD-PLGA-PEG-NPs	PLGA-PEG-diblock copolymer	1:5	$91.10 \pm 7.4$	$57.65 \pm 6.3$

**3.4. Morphological characterization:** To evaluate the influence of using different polymers for the fabrication of CVD-loaded NPs, the shape and surface attributes of CVD-loaded EC-NPs, -PEG-NPs and -PLGA-PEG-NPs were executed by using SEM. The SEM micrographs of CVD-loaded EC-NPs revealed that the produced nanoparticles were spherical in shape with smooth surface characteristics shown in **Fig. 4a & b**. Moreover SEM micrographs showed characteristics agglomerates of EC-NPs and few are in groups and fuse with each other. The agglomeration and fusing of EC-NPs might be attributed to their low surface charge which could result in particle aggregation and grouping. The approximate mean particle size of CVD-loaded EC-NPs showed by SEM micrograph was  $\sim 250$  nm which is considerably varied from the mean particle size obtained in size distribution scale ( $209 \pm 16$  nm) as shown in **Fig. 2a**. The larger mean particle size observed in SEM micrographs of EC-NPs might be attributed to some sort of particle agglomeration that can occur at lower zeta potential ( $-26.30 \pm -4.2$  mV) as shown in **Table 2**.

Additionally the characteristics shape and surface morphology of CVD-loaded PEG-NPs revealed tetragonal shape with smooth and regular surface characteristics as shown in **Fig. 4c and d**. The

approximate mean particle size of CVD-loaded PEG-NPs shown in SEM micrograph was  $\sim 220$  nm which is in correspondence with the mean particle size obtained in size distribution scale ( $229 \pm 26$  nm) as shown in **Fig. 2a**. Similarly SEM micrographs were also obtained for PLGA-PEG-NPs which are shown in **Fig. 4e and f**. The micrographs revealed a rounded shape with irregular surface morphology. Moreover the images obtained also showed characteristic curvatures on the surface of PLGA-PEG-NPs which might be attributed to the diblock co-polymerization of PLGA and PEG polymers. The mean particle size of CVD-loaded PLGA-PEG-NPs approximated in SEM micrographs was  $\sim 250$  nm which is in accordance with the mean particle size ( $253 \pm 19$  nm) observed in light scattering experiment.

In addition to that the PLGA-PEG-NPs were observed to be not agglomerated with each other as shown in **Fig. 4e and f**. This characteristics might be attributed to their higher surface charge ( $-54.26 \pm -7.2$  mV) and could result in optimum formulation stability of suspending particles in oral liquid dosage form on storage. The SEM micrographs revealed morphological diversity of CVD-loaded NPs by using different types of polymers as drug delivery system.



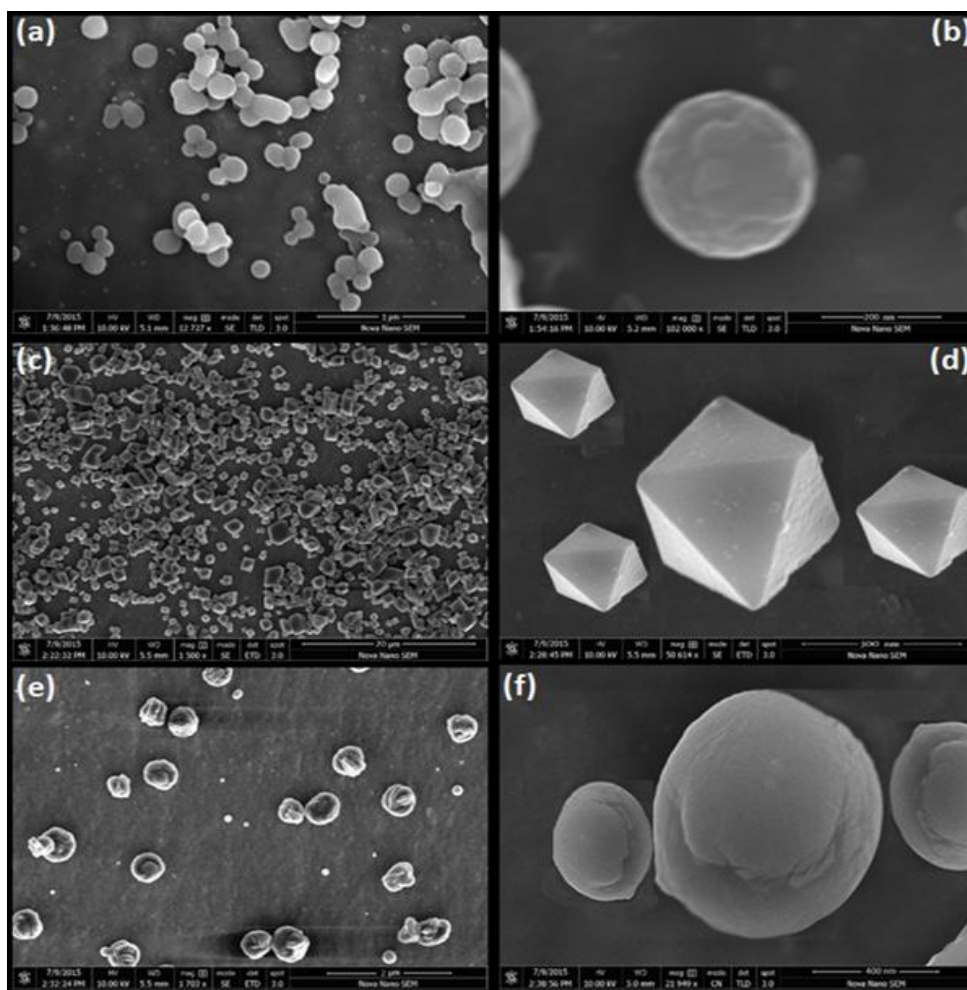


**FIG.4: EFFECT OF TYPE OF POLYMER USED IN THE PREPARATION OF CVD-LOADED NPs ON THE (a) CHARACTERISTIC SHAPE AND SURFACE MORPHOLOGY OF CVD-LOADED EC-NPs PREPARED AT 1:1 DRUG-TO-POLYMER MASS RATIO, (b) CHARACTERISTIC SHAPE AND SURFACE MORPHOLOGY OF CVD-LOADED PEG-NPs PREPARED AT 1:1 DRUG-TO-POLYMER MASS RATIO, (c) CHARACTERISTIC SHAPE AND SURFACE MORPHOLOGY OF CVD-LOADED PLGA-PEG-NPs PREPARED AT 1:1 DRUG-TO-POLYMER MASS RATIO.**

**3.4. FT-IR analysis:** The FT-IR spectra of pure CVD, EC, and CVD-loaded-EC-NPs are shown in **Fig.5A**. The results indicate that the intense characteristic peak of CVD appeared at  $3344\text{ cm}^{-1}$  and  $3298\text{ cm}^{-1}$  represent  $\text{-OH}$  stretching and  $\text{N-H}$  stretching vibrations, respectively. The characteristics peaks appeared at  $2912\text{ cm}^{-1}$  and  $2879\text{ cm}^{-1}$  ( $\text{-CH}$  stretching) and peaks recorded at  $1375\text{ cm}^{-1}$  and  $1450\text{ cm}^{-1}$  represented  $\text{CH}_2$  and  $\text{CH}_3$  bending vibrations respectively, in the CVD spectrum. The characteristics peak appeared in pure EC at  $3421\text{ cm}^{-1}$  indicate  $\text{-OH}$  stretching. Similarly, the peaks appeared at  $3092\text{ cm}^{-1}$  and  $2969\text{ cm}^{-1}$  indicate  $\text{-CH}$  stretching and peaks recorded at  $1365\text{ cm}^{-1}$  and  $1395\text{ cm}^{-1}$  represent  $\text{CH}_2$  and  $\text{CH}_3$  bending vibrations respectively. Result indicated that the characteristic peak appeared in the spectrum of CVD-loaded EC-NPs at  $3401\text{ cm}^{-1}$  representing  $\text{-OH}$  group (stretching vibration)

became broader and higher in intensity compared to EC ( $3344\text{ cm}^{-1}$ ), which indicated occurrence of hydrogen bonding between  $\text{-OH}$  bending groups of CVD at  $3344\text{ cm}^{-1}$  and EC at  $3421\text{ cm}^{-1}$ . In addition, the peak at  $1322\text{ cm}^{-1}$  ( $\text{C-N}$  bending) in the EC spectra shifted to  $1375\text{ cm}^{-1}$  in CVD-loaded EC-NPs spectra which indicates interactions between the  $\text{-C=O}$  group of EC and  $\text{-NH}$  group of CVD.

These results indicate that CVD was successfully loaded on to the EC-NPs. The cyclic ether ( $\text{C-O-C}$ ) showed broad distinctive peak near  $1100\text{ cm}^{-1}$  also appeals the possible interaction between EC and CVD. Moreover, the FT-IR spectrum of CVD-loaded EC-NPs showed several mix peaks showing drug is well distributed throughout the polymer matrix<sup>24</sup>.

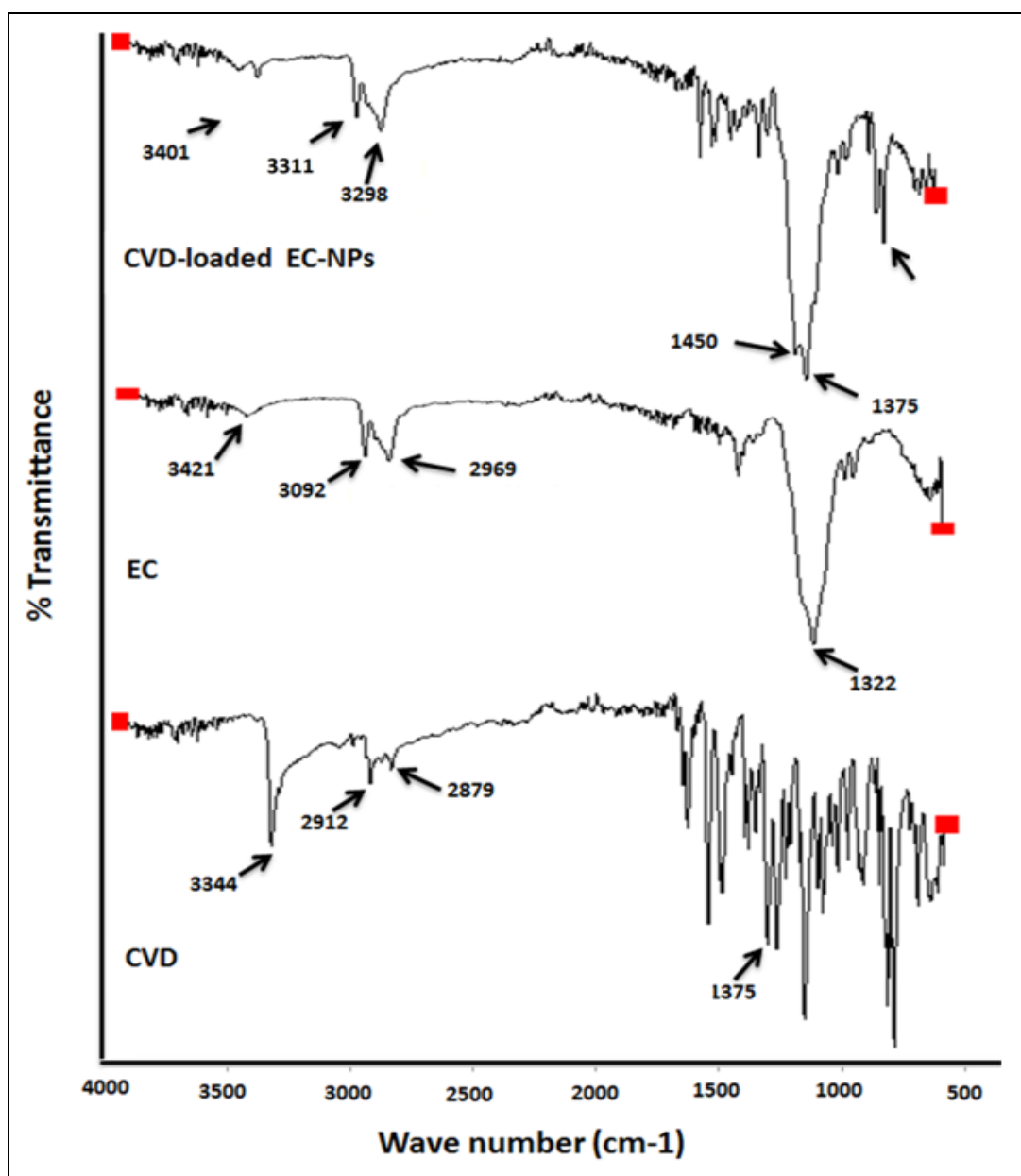


FIG.5A: FT-IR SPECTRA OF CVD, EC, AND CVD-LOADED EC-NPs.

The FT-IR spectra of pure CVD, PEG and CVD-loaded PEG-NPs have been shown in Figure 5B. In the spectrum of pure CVD, the intense characteristic peak appeared at  $3344\text{ cm}^{-1}$  and  $3298\text{ cm}^{-1}$  represented  $\text{-OH}$  stretching and  $\text{N-H}$  stretching vibrations, respectively. Other characteristics peaks appeared at  $2912\text{ cm}^{-1}$  and  $2879\text{ cm}^{-1}$  indicate  $\text{-CH}$  stretching and peaks recorded at  $1375\text{ cm}^{-1}$  and  $1450\text{ cm}^{-1}$  represented  $\text{CH}_2$  and  $\text{CH}_3$  bending vibrations respectively, in the CVD spectrum. The absorption band observed in the spectrum of PEG 8000 were appeared at  $3401\text{ cm}^{-1}$  and  $2878\text{ cm}^{-1}$  indicate  $\text{-OH}$  stretching and  $\text{C-H}$  stretching. The characteristics peak appeared at  $1464\text{ cm}^{-1}$  represent  $\text{C-H}$  bending.

Similarly, the peaks appeared at  $1094\text{ cm}^{-1}$  indicate  $\text{C-O-H}$  stretching. Result indicated that the characteristic peak appeared in the spectrum of CVD-loaded PEG-NPs at  $3301\text{ cm}^{-1}$  representing  $\text{-OH}$  group (stretching vibration) became broader and higher in intensity compared to PEG ( $3401\text{ cm}^{-1}$ ), which indicated occurrence of hydrogen bonding between  $\text{-OH}$  groups of CVD at  $3344\text{ cm}^{-1}$  and PEG at  $3401\text{ cm}^{-1}$ . The FT-IR spectrum of CVD-loaded PEG-NPs showed mix peaks of CVD and PEG 8000, indicated polymeric interaction to the CVD<sup>25</sup>.

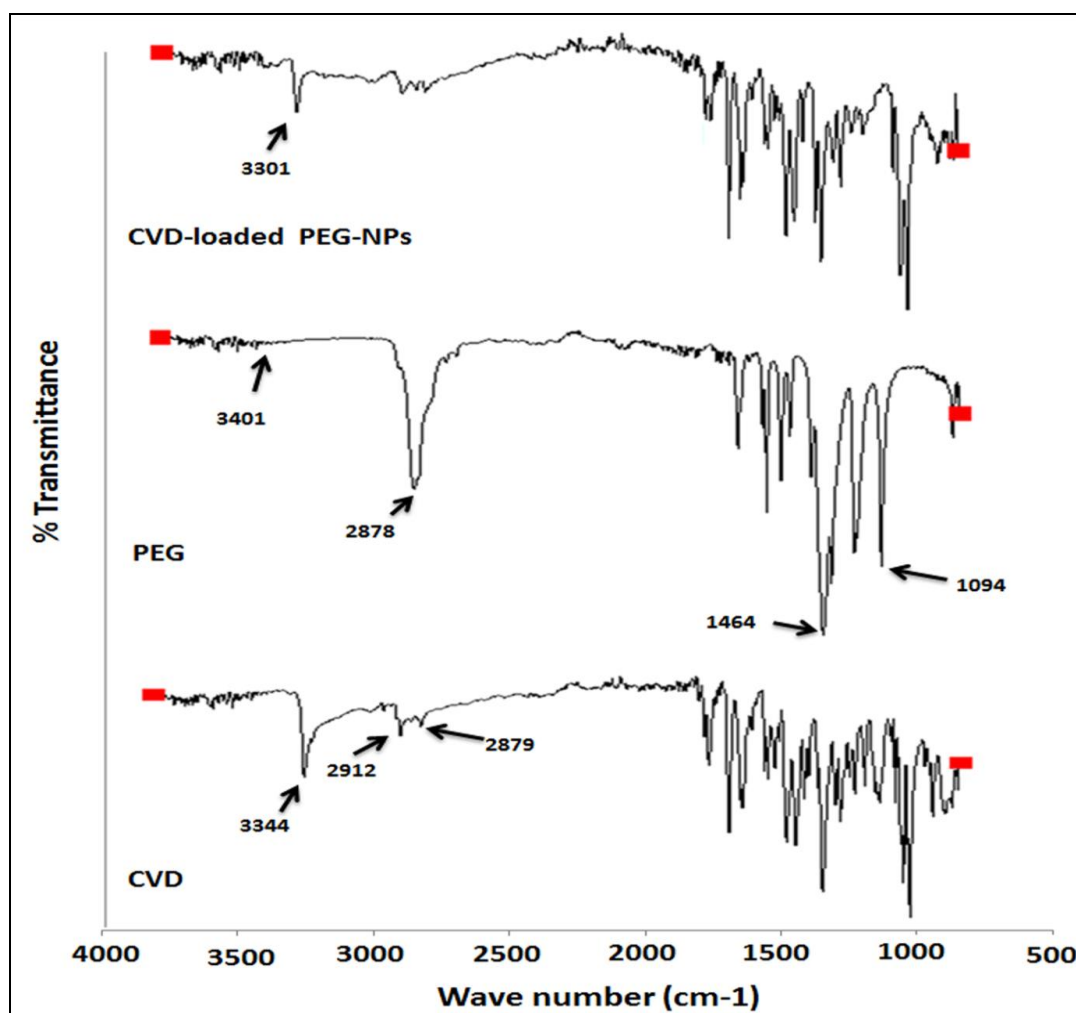


FIG.5B: FT-IR SPECTRA OF CVD, PEG, AND CVD-LOADED PEG-NPs.

The FT-IR spectra of pure CVD, PEG and CVD-loaded PEG-NPs have been shown in Fig.5C. In the spectrum of pure CVD, the intense characteristic peak appeared at  $3344\text{ cm}^{-1}$  and  $3298\text{ cm}^{-1}$  represented  $\text{-OH}$  stretching and  $\text{N-H}$  stretching vibrations, respectively. Other characteristics peaks appeared at  $2912\text{ cm}^{-1}$  and  $2879\text{ cm}^{-1}$  indicate  $\text{-CH}$  stretching and peaks recorded at  $1375\text{ cm}^{-1}$  and  $1450\text{ cm}^{-1}$  represented  $\text{CH}_2$  and  $\text{CH}_3$  bending vibrations respectively, in the CVD spectrum.

The absorption band observed in the spectrum of PEG 8000 were appeared at  $3401\text{ cm}^{-1}$  and  $2878\text{ cm}^{-1}$  indicate  $\text{-OH}$  stretching and  $\text{C-H}$  stretching. The characteristics peak appeared at  $1464\text{ cm}^{-1}$  represent  $\text{C-H}$  bending. Similarly, the peaks appeared at  $1094\text{ cm}^{-1}$  indicate  $\text{C-O-H}$  stretching. The pure PLGA sample showed peaks in the spectral region of  $2850\text{-}2500\text{ cm}^{-1}$  indicate  $\text{-CH}$ ,  $\text{-CH}_2$ , and  $\text{-CH}_3$  stretching vibration, Moreover, the intense characteristics peaks appeared in the

spectral region of  $1700\text{-}1800\text{ cm}^{-1}$  represent  $\text{-C=O}$  stretching vibration and those appeared in  $1050\text{-}1250\text{ cm}^{-1}$  indicate  $\text{C-O}$  stretching (Mainardes et al., 2006). The FT-IR spectra of pure PLGA had also shown  $\text{-OH}$  stretching vibrations ( $3200\text{-}3500\text{ cm}^{-1}$ ). Result indicated that the characteristic peak appeared in the spectrum of CVD-loaded PEG-NPs at  $3418\text{ cm}^{-1}$  representing  $\text{-OH}$  group (stretching vibration) became broader and higher in intensity compared to pure PEG ( $3401\text{ cm}^{-1}$ ) and PLGA, which indicate occurrence of hydrogen bonding between  $\text{-OH}$  groups of CVD at  $3344\text{ cm}^{-1}$ , PEG at  $3401\text{ cm}^{-1}$  and PLGA. The FT-IR spectrum of CVD-loaded PLGA-PEG-also showed many absorption peaks overlapped with pure CVD, PEG, and pure PLGA. It can be concluded that no strong chemical interaction occurred between drug and polymer; however, a polymeric interaction occurred between drug and polymers.

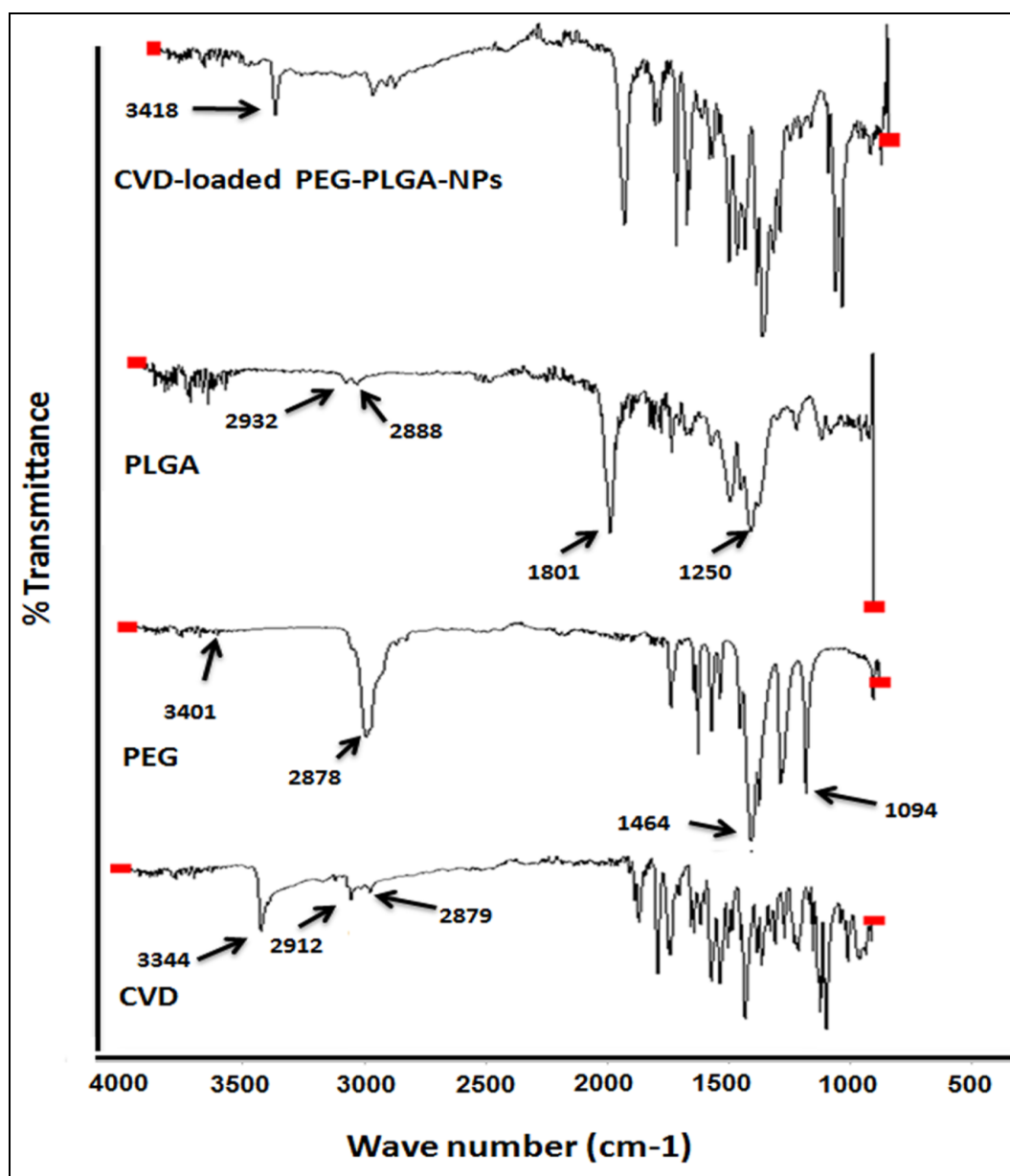


FIG.5C: FT-IR SPECTRA OF CVD, PEG, PLGA, AND CVD-LOADED PLGA-PEG-NPs.

**3.5. *In vitro* release profile:** *In vitro* drug release studies were carried out to evaluate the pattern of CVD release from CVD-loaded EC-, PEG- and PLGA-PEG-NPs compared to the pure CVD. Resulting data obtained is presented in Figure 6. A series of *in vitro* dissolution experiments were conducted using phosphate buffer at various pHs such as at 1.2, 6.8, and distilled water at  $37 \pm 2$  °C for 24 h. It was observed that the release behavior of CVD from the polymeric matrix of CVD-loaded EC-NPs, PEG-NPs, and PLGA-PEG-NPs exhibited biphasic pattern characterized by a fast initial release during the first 10 min followed by a slower and continuous release of drug as shown in **Fig.6** (A1). Similar release pattern has also been previously observed from other PLGA polymeric

systems<sup>26, 27</sup>. The burst release of drugs might be due to the dissolution and diffusion of the drug that was poorly entrapped in the polymer matrix, while the slower and continuous release may be attributed to the diffusion of the drug localised in the EC-/PEG-/PLGA-PEG- core of the NPs. The authors further noticed that the rate of CVD release from the polymeric matrix of NPs was varied with pH of dissolution media. The fast and highest amount of drug was released from CVD-loaded EC-NPs at acidic pH (>80%) within 10 min, which might predispose the maximum release of drug in gastric lumen after an oral administration of CVD-loaded polymeric NPs.



The authors also noticed that the rate and extent of CVD release was also greatly influenced by type of polymer used as drug delivery system. The highest percentage (>80%) of CVD was observed to be released from EC-NPs compared to PEG-NPs (approx. 50%) and PLGA-PEG-NPs (approx. 50%) in the acidic media (as shown in **Fig. 6(A1)**). Followed by an initial burst release at 10 min, the release rate of CVD became significantly slower until 24 h with an approximate release of 95% of CVD from EC-NPs compared with 85% from PEG-NPs and 65% from PLGA-PEG-NPs. The lowest release rate of CVD from PLGA-PEG-NPs revealed that this delivery system could efficiently protect CVD from occurring first pass metabolism and premature degradation occur by gastric milieu.

Similarly, the rate and extent of drug release from EC-NPs was also high in dissolution media at pH 6.8; however, an insignificant difference between EC-NPs and PLGA-PEG-NPs was observed with an approximate total release of 63% and 58% of CVD in 24 h, respectively (as shown in Figure 6B2 and C2). The significant increase in the release of CVD from PLGA-PEG-NPs after about 12 h might be the result of diffusion of incorporated drug from the polymeric matrix that might increase the release rate significantly after 12 h. The higher releasing efficiency of PEG-NPs in distilled water might be the result of swelling of polymers, due to its hydrophilic nature, in distilled water and resulted increase in pore size of polymeric matrix. Almost a similar release pattern (biphasic release profile) was also observed from the *in vitro* release experiments of CVD-loaded EC-NPs, -PEG-NPs and -PLGA-PEG-NPs prepared at higher drug-to-polymer mass ratio (1:2.5) in acidic media as shown in **Fig. 6(B1)**.

It was observed that the highest amount of CVD (approx. 70%) was released from EC-NPs within first 10 min compared with PEG-NPs (approx. 40%) and PLGA-PEG-NPs (approx. 35%) at pH 1.2. Interestingly, the resulted data obtained with the drug-to-polymer mass ratio of 1:2.5 also revealed the lowest percentage of CVD release from PLGA-PEG-NPs as a function of time. The total percentages of CVD release from the EC-NPs (approx. 95%) and PEG-NPs (approx. 85%) were significantly lowered compared with PLGA-PEG-NPs (approx. 60%) after 24 h. The drug release

observed at pH 6.8 and distilled water was significantly (p80%) and 1:2.5 (approx. 70%) in acidic media within first 10 min. After an initial burst release, a gradual increase in the release rate of CVD was observed from all the nanoparticulate delivery system with an approx. release of 55% from EC-NPs and 50% from PEG-NPs compared with only 35% from PLGA-PEG-NPs at 24 h in acidic media. However the drugs release from all the polymeric NPs at all the pH was greatly higher compared to the release from bulk CVD.

Hence the results clearly expressed the efficiency of polymeric drug delivery systems in improving the solubility and dissolution of CVD compared to the rate of release from bulk drug. The rate and extent of CVD release from CVD-loaded EC-NPs, -PEG-NPs, and PLGA-PEG-NPs fabricated at 1:1 drug-to-polymer mass ratio was found to be considerably higher compared to 1:2.5 and 1:5. Authors observed that increase in drug to polymer ratio resulted in decreased releasing rate and extent as shown in **Fig. 6**. These results were also in agreement with previously published report<sup>28, 29</sup>. The resulted data also addressed that PLGA-PEG-NPs had shown the lowest release rate of CVD compared with EC-NPs and -PEG-NPs at acidic pH. A significantly lower percentage of drug release from PLGA-PEG-NPs; particularly prepared at 1:2.5 and 1:5 drug-to-polymer mass ratios could efficiently reduce the first pass metabolism and premature degradation of CVD by gastric milieu.

The slower release of CVD from PLGA-PEG-NPs could be due to the fact that PLGA is a hydrophobic polymer which might impart amphiphilic nature to PLGA-PEG-NPs [30]. The resulted data also revealed that the release rate of CVD from PLGA-PEG-NPs was increased at higher time points compared with PEG-NPs at pH 6.8 and distilled water. This might be the result of diffusion of incorporated drug from the polymeric matrix or due to the partial degradation of polymer. Notably, the dissolution rate and release profile of CVD was observed to significantly higher compare to the bulk drug. These results clearly elucidate that the rate and extent of drug dissolution were remarkably enhanced by fabricating CVD in NPs delivery system.

The enhanced dissolution rate of CVD-loaded NPs could be accredited to the marked decrease in particle size, larger surface area, increased

solubility, and the amorphous nature of the drug in the formulations<sup>1</sup>.

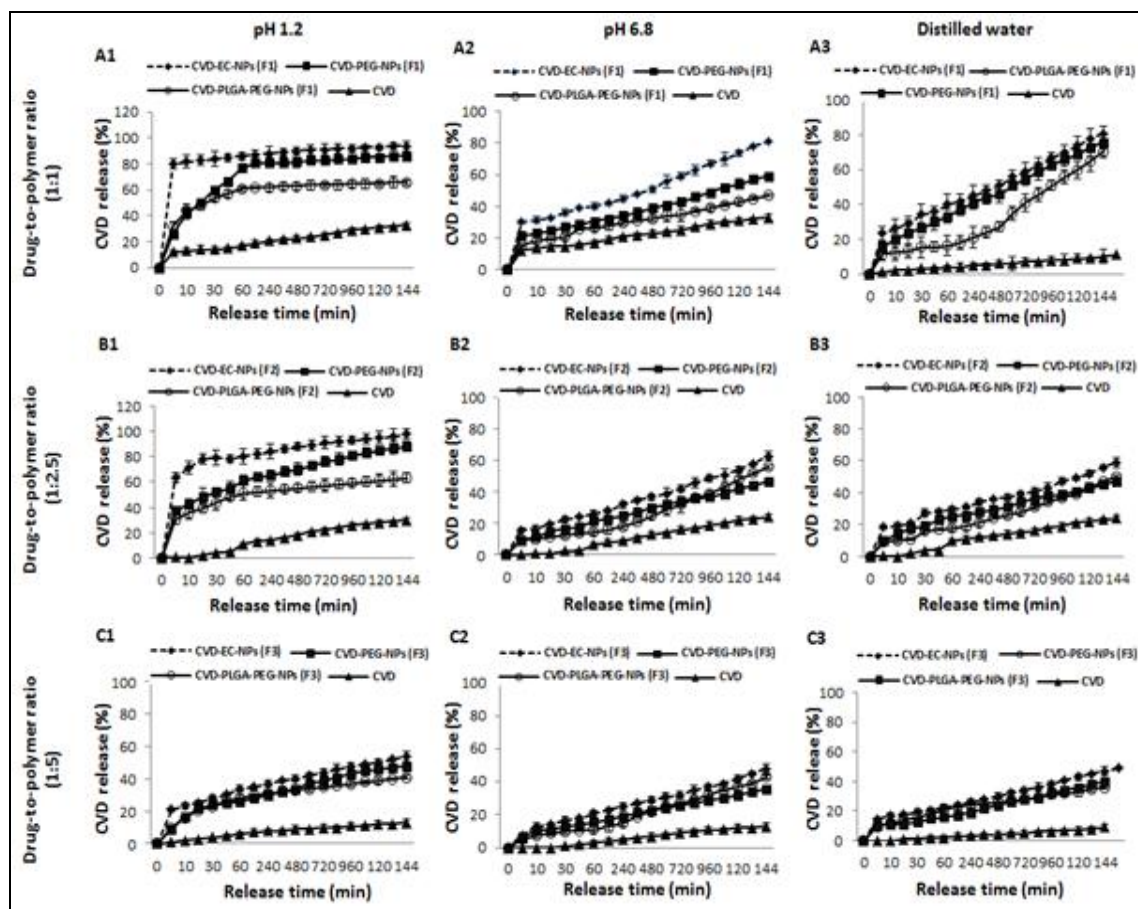


FIG. 6: EFFECTS OF DRUG-TO-POLYMER MASS RATIOS AND TYPES OF POLYMERS (EC, PEG AND PLGA-PEG) ON THE RELEASE PROFILE OF CVD FROM CVD-LOADED EC-NPs, -PEG-NPs, AND -PLGA-PEG-NPs AT PH 1.2 (A1, B1, C1), PH 6.8 (A2, B2, C2), AND IN DISTILLED WATER (A3, B3, C3). RESULTS WERE REPORTED AS MEAN  $\pm$  S.D.

**CONCLUSION:** The present study was aimed to investigate the impact of formulation parameters including drug-to-polymer mass ratios and types of polymers on the physicochemical characteristics and in vitro release behavior of CVD-loaded NPs. The resulted data clearly verified a significant influence of the formulation parameters on the mean particle size, zeta potential, size distribution index, %EE and %LC of CVD-loaded NPs. The SEM analysis also revealed conformational changes in the shape and surface characteristics from round smooth spherical to irregular tetragonal surface morphology varying with polymer type. Together the solubility and dissolution studies explored significantly higher rate and extent of CVD release from polymeric delivery systems compared to pure bulk drug. The resulted data also addressed that PLGA-PEG-NPs; particularly

prepared at 1:2.5 and 1:5 drug-to-polymer mass ratios could efficiently prevent the first pass metabolism and premature degradation of incorporated CVD occurred by gastric milieu. This study clearly identified the controlling parameters to fabricate CVD-loaded-NPs with optimal physicochemical characteristics and provide an opportunity of manipulating and optimizing the nanoparticles for intended pharmaceutical and nutraceutical applications.

**ACKNOWLEDGEMENT:** The authors gratefully acknowledge COMSATS Institute of Information Technology Abbottabad, Pakistan, Faculty of Chemistry, Lahore University of Management Sciences and Faculty of Pharmacy, Universiti Teknologi MARA for support and providing resources to write this article.

**DECLARATION OF INTEREST:** The authors report no declaration of interest in the current research work.

## REFERENCES:

- Xia D, Quan P, Piao H, Piao H, Sun S, Yin Y, Cui F. Preparation of stable nitrendipine nanosuspensions using the precipitation-ultrasonication method for enhancement of dissolution and oral bioavailability. *Eur J Pharm Sci* 2010; 40(4):325–334.
- Liu D, Xu H, Tian B, Yuan K, Pan H, Ma S, Yang X, Pan W. Fabrication of carvedilol Nano suspensions through the anti-solvent precipitation-ultrasonication method for the improvement of dissolution rate and oral bioavailability. *AAPS PharmSciTech* 2012a; 13: 295–304.
- Pu X, Sun J, Li M, He Z. Formulation of Nano suspensions as a new approach for the delivery of poorly soluble drugs. *Currnanosci* 2009; 5:417–427.
- Lee KS, Chung HC, Im SA, Park YH, Kim CS, Kim SB. Multicenter phase II trial of Genexol-PM, a Cremophor-free, polymeric micelle formulation of paclitaxel, in patients with metastatic breast cancer. *Breast Cancer Res Treat* 2008; 108:241–250.
- Kim DW, Kim SY, Kim HK, Kim SW, Shin SW, Kim JS. Multicenter phase II trial of Genexol-PM, a novel Cremophor-free, polymeric micelle formulation of paclitaxel, with cisplatin in patients with advanced non-small-cell lung cancer. *Ann Oncol* 2007; 18:2009–491 2014.
- Kim TY, Kim DW, Chung JY, Shin SG, Kim SC, Heo DS. Phase I and pharmacokinetic study of Genexol-PM, a cremophor-free, polymeric micelle formulated paclitaxel, in patients with advanced malignancies. *Clin Cancer Res* 2004; 10:3708–3716.
- Gu F, Zhang L, Teply BA, Mann N, Wang A, Radovic-Moreno AF. Precise engineering of targeted nanoparticles by using self-assembled biointegrated block copolymers. *Proc Natl AcadSci U S A* 2008; 105:2586–2591.
- Zhang L, Radovic-Moreno AF, Alexis F, Gu FX, Basto PA, Bagalkot V. Co-delivery of hydrophobic and hydrophilic drugs from nanoparticle–aptamer bioconjugates. *Chem Med Chem* 2007; 2:1268–1271.
- Farokhzad OC, Cheng J, Teply BA, Sherifi I, Jon S, Kantoff PW. Targeted nanoparticle- aptamer bioconjugates for cancer chemotherapy in vivo. *Proc Natl AcadSci USA* 2006; 103:6315–6320.
- Cheng J, Teply BA, Sherifi I, Sung J, Luther G, Gu FX. Formulation of functionalized PLGA–PEG nanoparticles for in vivo targeted drug delivery. *Biomaterials* 2007; 28:869–876.
- Rijcken CJ, Soga O, Hennink WE, van Nostrum CF. Triggered destabilisation of polymeric micelles and vesicles by changing polymers polarity: an attractive tool for drug delivery. *J Control Release* 2007; 120:131–148.
- Torchilin VP. Micellar nanocarriers: pharmaceutical perspectives. *Pharm Res* 2007; 24:1–16.
- Li Y, Pei Y, Zhang X, Gu Z, Zhou Z, Yuan W. PEGylated PLGA nanoparticles as protein carriers: synthesis, preparation and biodistribution in rats. *J Control Release* 2001; 71:203–11.
- Farokhzad OC, Cheng J, Teply BA, Sherifi I, Jon S, Kantoff PW. Targeted nanoparticle- aptamer bioconjugates for cancer chemotherapy in vivo. *Proc Natl AcadSci USA* 2006; 103(16):6315–6320.
- Fonseca C, Simoes S, Gaspar RE. Paclitaxel-loaded PLGA nanoparticles: preparation, physicochemical characterization and *in vitro* anti-tumoral activity. *J Control Release* 2002; 83(2):273–286.
- Planinšek O, Kovačič B, Vrečer F. Carvedilol dissolution improvement by preparation of solid dispersions with porous silica. *Int J Pharm* 2011a; 406: 41–48.
- Merisko-Liversidge E, Liversidge GG, Cooper ER. Nanosizing: a formulation approach for poorly-water-soluble compounds. *Eur J Pharm Sci* 2003; 18: 113–120.
- Hite M, Turner S, Federici C. Part 1: Oral delivery of poorly soluble drugs. *Pharmaceutical Manufacturing and Packing Sourcer*, 2003: 1–3.
- Papadimitriou SA, Achilias DS, Bikiaris DN. Chitosan-g-PEG nanoparticles ionically cross-linked with poly (glutamic acid) and tripolyphosphate as protein delivery systems. *Int J Pharm* 2012; 430:318–327.
- Dora CP, Singh SK, Kumar S, Datusalia AK, Deep A. Development and characterization of nanoparticles of glibenclamide by solvent displacement method. *Acta Pol Pharm* 2010; 67: 283-290.
- Jain S, Mittal AK, Jain AR, Mahajan R, Singh D. Cyclosporin A loaded PLGA nanoparticle: preparation, optimization, in-vitro characterization and stability studies. *CurrNanosci* 2010;6: 422–431.
- Pamulaparti S. Formulation of ibuprofen loaded ethyl cellulose nanoparticles by Nanoprecipitation technique. *Asian J Pharm Clin Res* 2014; 7(3):44–48.
- Mehta RC, Thanoo BC, Deluca PP. Peptide containing microspheres from low molecular weight and hydrophilic poly(d,l-lactide-co-glycolide). *J Control Release* 1996;41: 249–257.
- Parida P, Mishra SC, Sahoo S. FTIR Spectroscopic In-vitro Drug Interaction Study of Nifedipine Microsphere. *Int J Pharm Stud Res* 2012.
- Biswal S, Sahoo J, Murthy P. Characterisation of gliclazide-PEG 8000 solid dispersions. *Tropical Journal of Pharmaceutical Research* 2009;8(5):417–424.
- Feng SS, Huang GF. Effects of emulsifiers on the controlled release of paclitaxel (Taxol) from nanospheres of Biodegradable polymers. *J Control Release* 2001; 71:53–69.
- Wang YM, Sato H, Horikoshi I. In vitro and in vivo evaluation of taxol release from poly (lactic-co-glycolic acid) microspheres containing isopropyl myristate and degradation of the microspheres. *J Control Release* 1997; 49(2–3):157–166.
- Chella N, Yada KK, Vempati R. Preparation and evaluation of ethyl cellulose microspheres containing diclofenac sodium by novel w/o/o emulsion method. *J Pharm Sci Res* 2010; 2:884–888.
- Tsume Y, Amidon G, Takeuchi S. Dissolution effect of gastric and intestinal pH for BCS class II drug, pioglitazone: new in vitro dissolution system to predict in vivo dissolution. *J Bioequiv Availab* 2013b; 5:224–227.
- Yeo Y, Park K. Control of encapsulation efficiency and initial burst in polymeric microparticle systems. *Archives of pharmacol research* 2004; 27:1–12.

### How to cite this article:

Khan S, Ali W, Rahman NU, Shah SMM, Khan J, Shah SMH, Hussain Z: Self-assembled biodegradable polymeric nanoparticles with improved solubility of carvedilol: preparation, characterisation and *in vitro* release kinetics. *Int J Pharm Sci Res* 2016; 7(10): 3971-85.doi: 10.13040/IJPSR.0975-8232.7(10).3971-85.